COUPLING OF FINITE-VOLUME-METHOD AND INCOMPRESSIBLE SMOOTHED PARTICLE HYDRODYNAMICS METHOD FOR MULTIPHASE FLOW

CHRISTIAN A. WALTER, MANUEL HIRSCHLER AND ULRICH NIEKEN

Institute of Chemical Process Engineering, University of Stuttgart
Böblinger Straße 78, 70199 Stuttgart, Germany
christian.walter@icvt.uni-stuttgart.de, http://www.icvt.uni-stuttgart.de

Key words: SPH, FVM, coupling, multiphase, ISPH

Abstract. It is an intuitive way to use the advantages of two different simulation methods, such as the Finite-Volume (FV) and Smoothed Particle Hydrodynamics (SPH), to reduce the computational effort. Finite-Volume, like other grid-based methods, is advantageous for huge systems without fluid-fluid interfaces, whereas SPH is advantageous in the vicinity of fluid interfaces. We will present our first results for a combined simulation, including a moving SPH domain, in a simple Poiseuille flow and a more complex multiphase capillary rise scenario.

1 INTRODUCTION

Mesh-free simulation methods, as the Smoothed Particle Hydrodynamics method (SPH), are advantageous for simulating free-surface flows, solid-fluid interaction with deformations and multiphase applications. In contrast to grid-based methods, SPH doesn't require an expensive meshing or adaption of the grids. On the other hand, simulations of simple flow are very expensive. A way to reduce the computational effort of the SPH method is to use it only in parts of the problem domain where it is necessary. In other parts a more efficient calculation method, like the Finite-Volume method (FVM) may be used.
In the literature some work can be found for linking grid-based and grid-free simulation methods for solid-fluid systems [1] but there is a leak in coupling fluid-fluid systems [2]. Therefore, a new approach to combine both simulation methods for multiphase flow applications is presented. The coupling strategy is outlined using FVM and, in conformity, an incompressible SPH (ISPH) solver.

2 Coupling of Finite Volume Method an ISPH

2.1 ISPH Solver

At our institute, the ISPH solver "SiPER" is developed and used for different applications in multi-phase micro-flow in porous media and morphology evolution in fluid systems. We use the model described in detail in [4]. The coupling strategy is based on our previously published open boundary conditions as described in [3]. We basic algorithm is a Predictor-Corrector integration scheme, where we use a Bi-Conjugate Gradient method to solve the Pressure Poisson Equation (PPE) using the PETSc-library [7].

2.2 Finite Volume Solver

The FVM is implemented as 2D staggered grid solver according to [5] inside the existing SiPER code. It is implemented in the same structure as the SPH solver with a Predictor-Corrector integration scheme. The PPE is also solved using a Bi-Conjugate Gradient method of the PETSc-library. The code is limited to an equidistant grid.

2.3 Coupling Strategy

Set up of the simulation domain

The first step of the coupled simulation is to lay the equidistant grid of the FVM over the whole domain with the height H and length L. Inside of this domain the SPH domain is inserted on a random position x_{SPH} with its belonging length L_{SPH}. Due to the fact that the coupling is only done in one direction the height of the SPH domain is equal to the total domain height H. This setup can be seen in figure 1. The red lines indicate the coupling boundaries between the two simulation methods.
The FV grid cells behind the SPH domain will be deactivated, therefore we get two separated FV domains. In each domain we can calculate a fluid with different properties.

Coupling boundary condition

The relevant properties for the coupling are the velocity $\mathbf{v} = (u, v)$ and the pressure p. For a successful coupling the following four conditions at the interface between the methods have to be fulfilled

$$\mathbf{v}_I^{SPH} = \mathbf{v}_I^{FVM}, \qquad (1)$$
$$\nabla \mathbf{v}_I^{SPH} = \nabla \mathbf{v}_I^{FVM}, \qquad (2)$$
$$p_I^{SPH} = p_I^{FVM}, \qquad (3)$$
$$\nabla p_I^{SPH} = \nabla p_I^{FVM}. \qquad (4)$$

Terms of higher order are neglected. Due to the properties of the Navier-Stokes equations, a Dirichlet (Eq. (1) or (3)) and a Neumann (Eq. (2) or (4)) boundary condition is needed. The incompressibility of the fluid fulfills condition (2). As second boundary condition a Dirichlet boundary for the pressure is chosen. The pressure at the interface is unknown
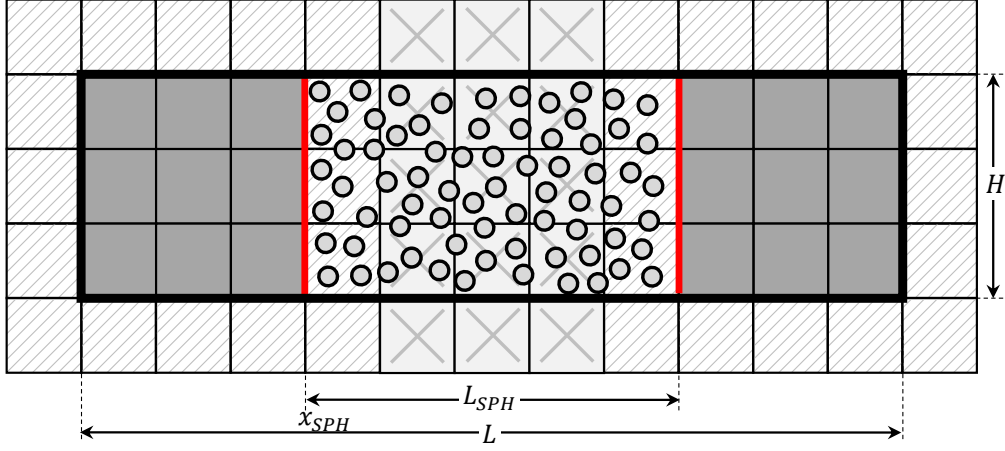
Figure 1: Setup of the simulation domain for the coupling of the FV ans SPH method.

a priori because of the random position of the SPH domain inside the whole simulation domain. Because of that we need to calculate the pressure for the Dirichlet boundary conditions iteratively.

At the interface in the SPH domain, the pressure p_I^{SPH} is calculated with an interpolation of the pressure values of the adjacent FV cells as shown in fig. 2 (right). At the interface in the FV domain, the pressure in the center of the boundary cells are needed. At this position a fictive SPH particle is inserted and with the SPH interpolation scheme the pressure can be calculated as shown in figure 2 (left). The pressure on the interface is calculated as

$$p_I^{FVM} = \frac{(p_r + p_i)}{2} \tag{5}$$

Obviously, with this approach the pressure on the interface has to be iterated until $p_I^{FVM} = p_I^{SPH}$. This pressure iteration takes part during the SPH corrector step.

Overlapping of the simulation domains

By using open boundary pressure conditions, small errors in the pressure solution are present. These errors prevent a convergence of the pressure iteration. To avoid this problem the simulation domains of SPH and FV will be slightly overlapped, as shown in fig. 3. The position of the interface is not equal to the boundary of each simulation domain but is defined as

$$x_I = \frac{x_{I,SPH} + x_{I,FVM}}{2}. \tag{6}$$

The pressure calculation for the FV boundary condition is now at a position with a negligible error. The iteration is aborted by two different criteria. First, the mean square
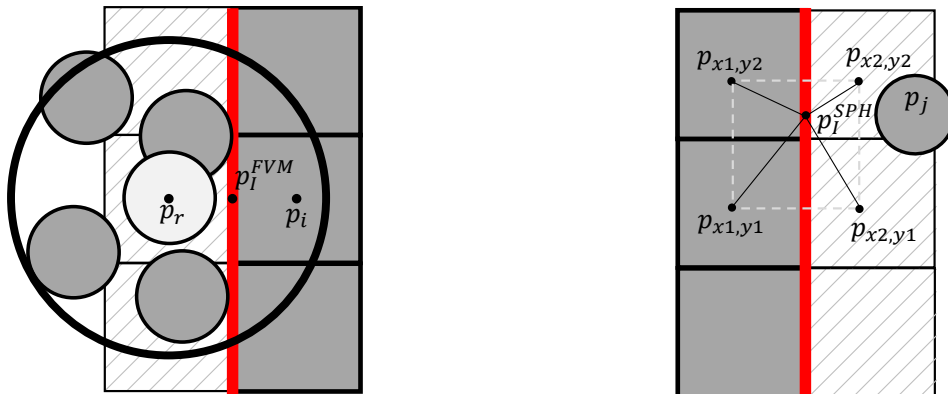
Figure 2: Pressure calculation at the interface for FV (left) with an SPH interpolation. Bilinear interpolation of the pressure on the grid cells for the SPH method (right)

deviation at the position of the interface x_I between the SPH and the FV pressure is used, second the variation of the pressure at the boundaries is used.
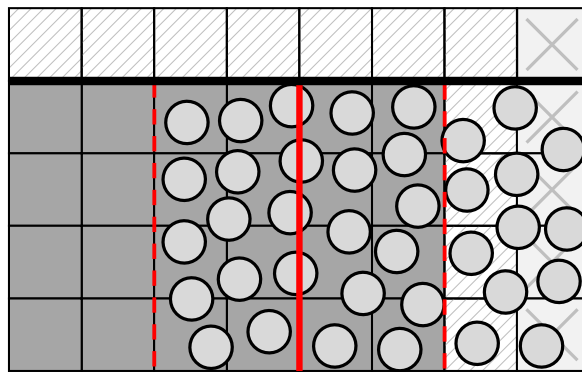

Figure 3: Interface with overlapping simulation methods.

Movement of the SPH domain

The aim of the coupling is to simulate e.g. bubbles in a bubble column where small, moving areas of multiphase flow are present. Therefore the SPH domain has to move inside the FV domain. To achieve this, the position of the SPH domain has to be calculated in every time step. This is done by identifying the phase boundary and then move the SPH domain in a way that the phase boundary is always in the center of the SPH domain. During this movement particles are generated or deleted as described for open boundary conditions in [4]. The FV grid will change due to the position of the SPH domain and grids will be deactivated or activated, applying the new fluid properties. The movement of the SPH domain is limited to one size of the grid cell per time step to avoid errors.

3   Results and discussion

3.1   Poiseuille Flow

A single-phase, two-dimensional Poiseuille flow is calculated for a viscous fluid with a density of $\rho = 1000\,^{kg}/_{m^3}$, a dynamic viscosity $\mu = 0.01\,^{kg}/_{s\,m}$ and a simulation domain with the height of $H = 1\,\text{mm}$ and the length $L = 6\,\text{mm}$. Dirichlet pressure conditions ($p_L = 180\,\text{Pa}$, $p_R = 0\,\text{Pa}$) are applied. A sketch up is shown in fig. 4.
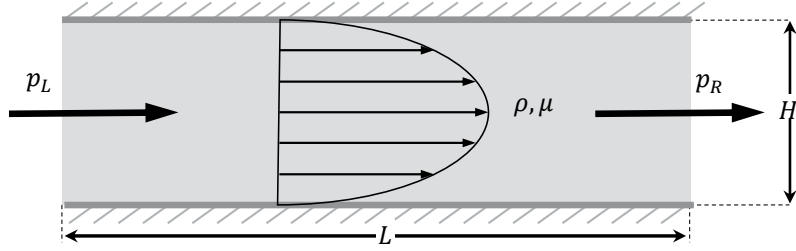
Figure 4: Visualization of the Poiseuille flow.

The solution of the velocity is compared to the analytic solution

$$
u_x\left(y,t\right) = \frac{g_x\,\rho}{2\,\mu}y\left(y-H\right) + \sum_{n=0}^{\infty}\frac{4\,g_x\,\rho\,H^2}{\mu\,\pi^3}\left(2n+1\right)^3
$$
$$
\sin\left(\frac{\pi\,y}{H}\left(2n+1\right)\right)\,exp\left(-\frac{\left(2n+1\right)^2\pi^2\mu}{\rho\,H^2}t\right).
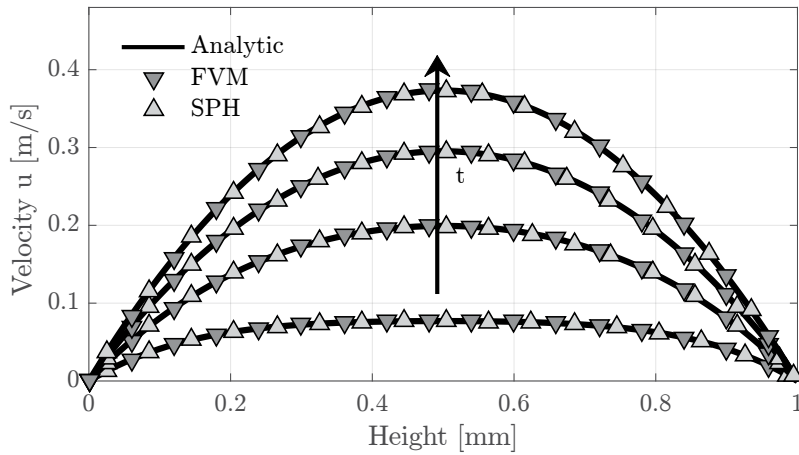$$
(7)

Figure 5: Comparison of the analytic velocity profile with the solution of the coupled simulation for four different points of time.

Figure 5 shows the calculated velocity at the left interface. The results are in good agreement with the analytic solution. The integrated error of pressure and velocity is below 0.1% at every time step.

3.2 Moving Poiseuille Flow

To evaluate the error of the moving SPH domain inside the FV domain, the SPH domain is moved multiple times from left to right and back again. This movement results in a triangle shaped pressure profile over the time as seen in fig. 6. The simulation
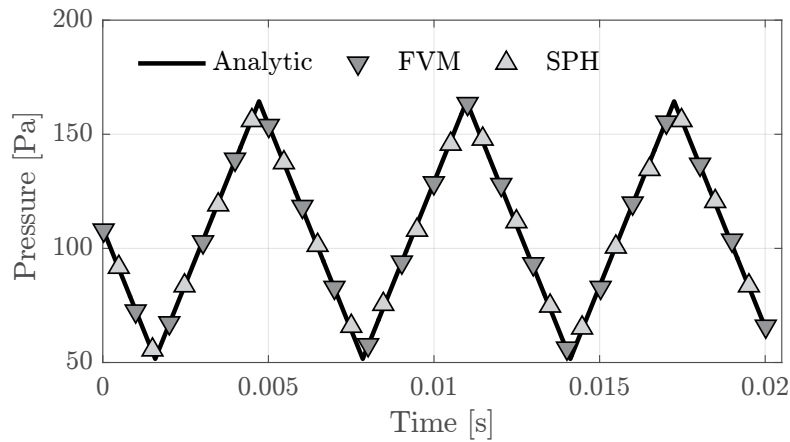
Figure 6: Pressure profile at the interface for a moving SPH domain.

represents the analytic solution very well. As seen in fig. 7, the error in the velocity through the movement is equally. In summary, it can be stated that the movement of the SPH domain does not result in a highly increasing error.
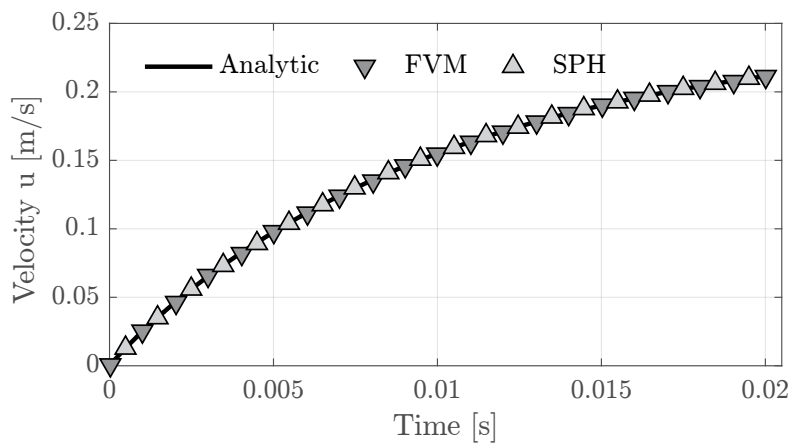
Figure 7: Temporal progress of the velocity at the interface.

3.3 Capillary Rise

A capillary rise between two flat parallel walls as shown in fig. 8 consists of a wetting fluid (w) ($\rho_w = 1800\,\mathrm{kg/m^3}$ $\mu_w = 0.0047\,\mathrm{kg/sm}$) and a non-wetting fluid (n) ($\rho_n = 1000\,\mathrm{kg/m^3}$ $\mu_n = 0.001\,\mathrm{kg/sm}$). The height of the simulation domain is $H = 9.3\,\mathrm{mm}$ and the distance between the two plates is $d = 1.55\,\mathrm{mm}$. The wetting fluid will move up through the capillary and stops on a stationary level (h_w) where the forces are in an equilibrium [6]. At the beginning the pressure sinks fast and ends on a stationary profile. Fig. 9 shows
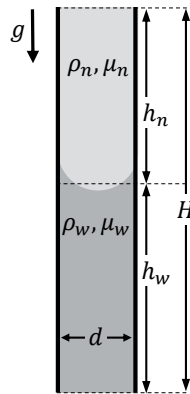

Figure 8: Visualization of the capillary rise.

the expected behavior for the pressure during the rise. Both interfaces between SPH and FV are shown, and the difference between both lines gives the pressure drop at the fluid fluid boundary. The results are in good agreement with capillary rise experiments [6].
We conclude that our coupling strategy leads to reasonable results. In future work, some minor issues at the interface between FVM and SPH need to be fixed. A promising alternative to match the interfaces is very recently presented by Napoli et al. [2].
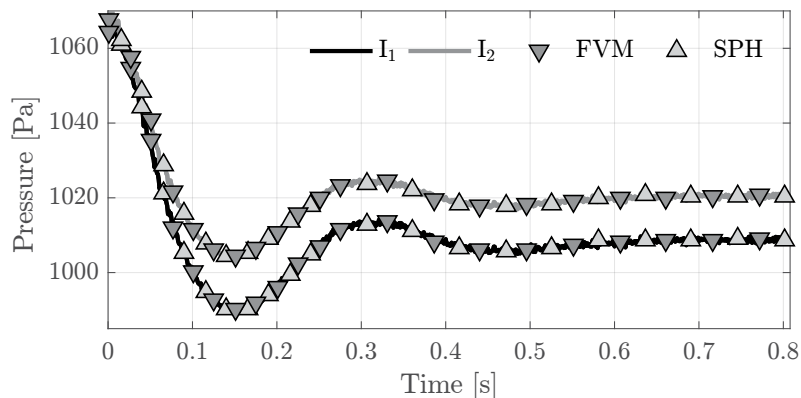

Figure 9: Temporal progress of the pressure for both interfaces.

916

REFERENCES

[1] Johnson, Gordon R. *Linking of Lagrangian particle methods to standard finite element methods for high velocity impact computations.* Nuclear Engineering and Design, 150(2):265 - 274, 1994.

[2] Napoli, E.; De Marchis, M.; Milice, B. and Monteleone, A. *A coupled Finite Volume-Smoothed Particle Hydrodynamics method for incompressible flows.* Computer Methods in Applied Mechanics and Engineering, 310:674 - 693, 2016.

[3] Kunz, P.; Hirschler, M.; Huber, M. and Nieken, U. *Inflow/outflow with Dirichlet boundary conditions for pressure in ISPH*, Journal of Computational Physics, Volume 326, 1 December 2016, Pages 171-187.

[4] Hirschler, M. et al. *Open boundary conditions for ISPH and their application to micro-flow*, Journal of Computational Physics, Volume 307, 15 February 2016, Pages 614-633.

[5] Griebel, M.; Dornseifer, T. and Neunhoeffer, T. *Numerical Simulation in Fluid Dynamics: A Practical Introduction.* SIAM e-books. Society for Industrial and Applied Mathematics (SIAM, 3600 Market Street, Floor 6, Philadelphia, PA 19104), 1997.

[6] Kunz, P.; Zarikos, I. M.; Karadimitriou, N. K.; Huber, M.; Nieken, U. and Hassanizadeh, S. M. (2016) *Transport in Porous Media*, volume 114, issue 2, pp. 581 - 600.

[7] Balay, S.; Abhyankar, S.; Adams, M. F.; Brown, J.; Brune, P.; Buschelman, K.; Dalcin, L.; Eijkhout, V.; Gropp, W. D.; Kaushik, D.; Knepley, M. G.; Curfman McInnes, L.; Rupp, K.; Smith, B. F.; Zampini, S. and Hong Zhang, H. (2016) *PETSc Web page*, http://www.mcs.anl.gov/petsc